in silico Plants, 2026, 8, diag004
https://doi.org/10.1093/insilicoplants/diag004
Published: 11 February 2026
Original research

in silico Plants OXFORD

Validation of root hair upscaling in rhizosphere solute transport models

Christian W. Kuppe [1]*, Andrea Schnepf [2], Johannes A. Postma [1]

[1]Forschungszentrum Jülich GmbH, Institute of Bio- and Geosciences – Plant Sciences (IBG-2), Jülich 52425, Germany
[2]Forschungszentrum Jülich GmbH, Institute of Bio- and Geosciences – Agrosphere (IBG-3), Jülich 52425, Germany

*Corresponding author. Forschungszentrum Jülich GmbH, Institute of Bio- and Geosciences – Plant Sciences (IBG-2), Jülich 52425, Germany.
E-mail: c.kuppe@fz-juelich.de

Abstract

Rhizosphere models are typically 1D radial symmetric with the root as a boundary condition and root hairs as a reaction term (source/sink term). This rhizosphere representation comprises a model reduction for solute transport from 3D to 1D, which upscales the geometry of the root hairs. Further reduction is common in root architectural models, representing the root as point-sinks in a numerical mesh. We validated whether upscaling root hair geometry results in model-errors for nutrient uptake. We compared three levels of rhizosphere model reduction with varying geometric representation: (1) a 3D model with diffusion around root hairs, solved with a finite element method; (2) a 1D radial model with root hairs as sink term; (3) the root as point-sink. We investigated four different cases: short-thick-coarse, long-thick-coarse, short-thin-dense, and long-thin-dense root hairs. Each case was investigated for ammonium and phosphorus. In most cases, 1D and 3D solutions are close together, indicating that the 1D model reduction is valid. The 1D simulations deviate from 3D for slowly diffusing phosphorus taken up by long, thick, coarse root hairs; however, this is an extreme scenario and shows a theoretical limit. Further reducing the root to a point sink only estimates uptake for the ammonium scenario, which has fast diffusion. The root point sink is sensitive to the mesh resolution. Representing root hairs or roots by sink terms works for small radii or fast diffusing solutes. The 1D radial models can give valid and computationally fast results, but further reduction can lead to errors.

Keywords: Rhizosphere model, cylindrical root, root hairs, finite element method (FEM), open-source Julia code, model order reduction, nutrient uptake

1. Introduction

Rhizosphere models are commonly used to simulate ion transport in the rhizosphere, nutrient uptake, and root exudation. The uptake rate is dependent on the nutrient concentration at the root surface. The nutrient concentration at the root surface further depends on diffusion and sorption in the rhizosphere. Root hairs extend the surface area of the root and soil exploration as they expand into the rhizosphere. Hence, the root hair can intercept nutrient uptake and influence the diffusion profile around the root. Root surface area and root hairs that are closely positioned to each other may compete for the same nutrients. The competition among root hairs was shown to depend on root hair geometric parameters like root hair density and length (Ma et al. 2001).

Instead of representing the rhizosphere in 3D, with the root and root hair surface explicitly representing geometrical boundaries, rhizosphere models are usually defined in 1D radial coordinates (reviewed by Kuppe et al. 2022b). The 1D radially symmetric model represents a rhizosphere cross section where nutrient uptake is uniform around the root. Rhizosphere models have been applied beyond their own scale. Such nutrient uptake per unit root length has been integrated up to the whole root system using either root growth functions (Cushman 1979, Barber and Cushman 1981, Kuppe et al. 2022a), taking into account the demography of the root system (additional root length, grown at later time points, has an uptake profile from a young rhizosphere), or root architectural models, to account for both demography and the spatial distribution of roots and soil conditions (Postma et al. 2017, Schnepf et al. 2018). The latter is achieved by discretizing the root system into segments and computing uptake by every root segment (e.g. Gonzalez et al. 2021). This, however, does not represent the soil as a continuum, and so further model

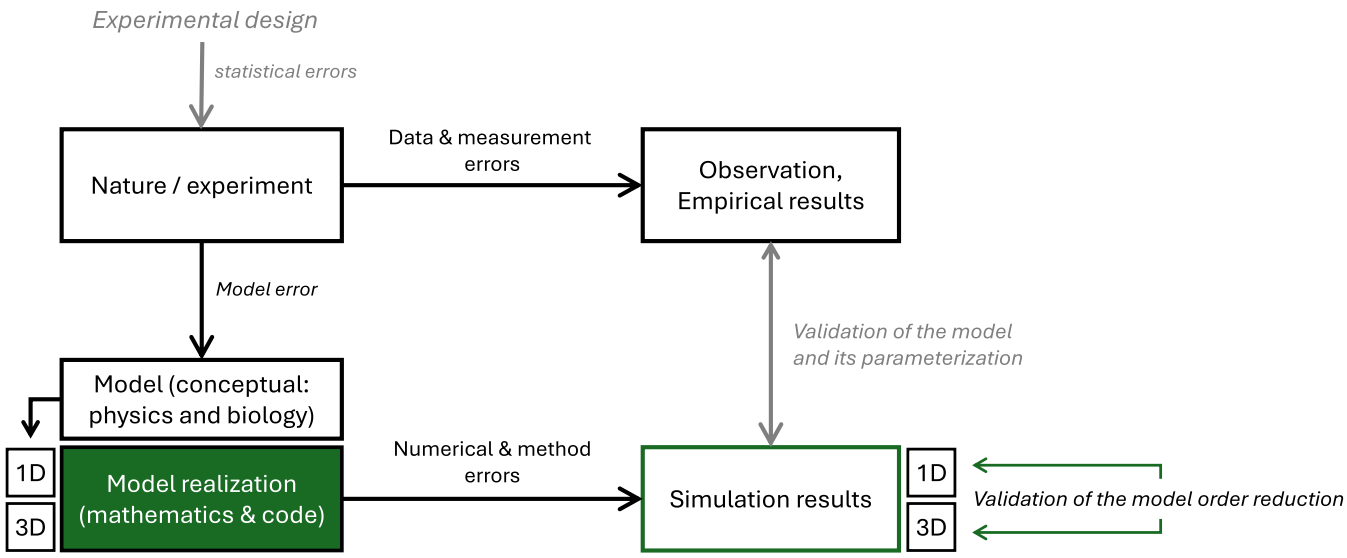

Figure 1 Model development and calibration face different sources of uncertainty. This study considers 1D approximations of the idealized 3D model of a root segment with hairs.

reduction is common where roots become sink terms in 1D, 2D, or 3D representations of the soil domain (Tournier Hecht and Comte 2015) and root-soil couplings in which rhizosphere models can be used to compute the sink term (Schnepf Leitner and Klepsch 2012, Mai et al. 2019, Schnepf et al. 2023). A root system consists of many segments, such that systematic errors in the solutions of the rhizosphere models can accumulate. The 1D radially symmetric model has been also used in crop models (e.g. Mollier et al. 2008).

As rhizosphere research is expanding rapidly, rhizosphere models will become more important for studying the complex interplay between root and soil physical, chemical and biological processes. Accurate representation of root rhizosphere processes, supposing correct scale integration to the whole root system, is crucial for drawing reliable conclusions. We ask if the model reductions described above, from 3D to 1D rhizosphere and further from a root as boundary condition to a 0D root-sink, are valid.

In the past, radial rhizosphere models were validated by comparing simulation results to experimental data for potassium (Claassen and Barber 1976, Claassen Syring and Jungk 1986) and phosphorus uptake (Itoh and Barber 1983, Macariola-See Woodard and Schumacher 2003). However, model parameters might have been obtained by calibration, which could potentially hide numerical errors (Fig. 1). Meanwhile, it became computationally feasible to compare model realizations with an explicit 3D simulation. The focus of this study is the representation of root hairs in nutrient uptake models. We validate the representation of the rhizosphere as 0D and 1D radial model with root hairs as a reaction term in the continuity equation (Baldwin Nye and Tinker 1973, Bhat Nye and Baldwin 1976) against a 3D representation of geometric root hairs having a volume. Thus, we validate the assumptions that underlie the model order reduction within the specific context of the given parameter ranges.

Geelhoed et al. (1997) compared the zero-sink phosphate uptake between two models and showed a difference of <15% after 10 d. In these 1D and 3D models, the root hair volume was not modelled geometrically and assumed not to influence diffusion. They avoided inter-root competition by using a 'large' rhizosphere domain. The 3D model was solved using finite differences. Hence, a 'line-method' yields a system of ordinary differential equations (ODEs) in time, which was solved with the implicit Gear's method of order 5. With these simplifications, Geelhoed et al. (1997) did not provide a full answer to the question of whether a 3D to 1D reduction is valid or if the volume of root hairs influences the diffusion and uptake of nutrients.

A comparison of a 1D analytical solution to a whole 3D root system has been performed for uptake of phosphorus using the commercial software Comsol with a finite element method (FEM) (Schnepf and Leitner 2009, Leitner et al. 2010b). Other root hair models were based on an image-based approach (Keyes et al. 2013, Daly et al. 2016), also using Comsol to simulate 3D root and root hairs on a computational cluster (Ruiz et al. 2020, Williams et al. 2022). Ruiz et al. (2020) investigated the impact of root hairs on phosphorus uptake from precipitation, high and low phosphorus concentrations, and gradients along the soil profile. A key part of their methodology is image processing to get a mesh from the X-ray CT scans. The authors provide Comsol mesh files (.mph), which either requires a Comsol licence or a conversion to a readable format. Since many open-source FEM simulation tools and libraries can handle Gmsh meshes well, we chose an open format for the simulations. Instead of a specific CT scan, we take the idealized 3D root geometry on which the 1D model is based to be able to make a statement about the model reduction and have models that rely on simple parameterization rather than expensive and context-dependent CT imaging.

Here, we compare the root hair model representations in the rhizosphere of a root segment (Fig. 1): i.e. the 1D upscaling of root hairs as a reaction term in the solute transport equation to a 3D model with volumetric root hair geometry to validate such model reduction. Some root architectural models implement roots as local sinks in the soil; therefore, we were interested in how far a root geometry can be simplified. Hence,

we additionally simulated nutrient uptake by the root and root hairs as a 0D point sink in the transport equation to investigate the limits of model reduction. We compare longer simulation times relevant to plant growth. We ask whether the root hair volume in the rhizosphere influences the diffusion of solutes enough that the 3D version is preferable over the 1D radial model for uptake (Ma et al. 2001). We ask under what conditions the 3D geometry differs strongly from the 1D and 0D realizations. We are interested in whether diffusion around root hairs influence uptake in a way that justifies a 3D modelling approach. Last, we ask whether the accuracy of our numerical simulations varies over time. Hence, we investigated the relative differences to our reference simulation over time.

2. Methods

2.1 Transport in the rhizosphere in 3D: from strong to weak formulation

Consider a three-dimensional rhizosphere domain $\Omega \subset \mathbb{R}^3$ and a boundary $\Gamma = \partial\Omega$, with $\Gamma = \Gamma_s \cup \Gamma_r$, for the outer (soil) and inner (root and root hair) boundaries. The strong form of transient diffusion of a substance with concentration in soil C: $\mathbb{R}^3 \times [0, T] \to \mathbb{R}$ is

$$\frac{\partial C}{\partial t} - \operatorname{div}(\boldsymbol{q}) = f \quad \text{in } \Omega \times (0, T] \tag{1}$$

$$\boldsymbol{q} \cdot \mathbf{n} = 0 \quad \text{on } \Gamma_s \times (0, T] \tag{2}$$

$$\boldsymbol{q} \cdot \mathbf{n} = q^* \quad \text{on } \Gamma_r \times (0, T] \tag{3}$$

$$C_l(., 0) = C_0 \quad \text{in } \Omega, \tag{4}$$

where the concentration $C = bC_l$, with soil buffer power b and concentration of substance in soil solution C_l. The flux by diffusion is

$$\boldsymbol{q} = D_e \nabla C, \tag{5}$$

where $D_e = D_l \theta\tau / b$ is the effective diffusion of the solute in soil that adjusts the diffusion in water, D_l, with the soil tortuosity, τ, and the soil buffer power, b, scaled by the volumetric water content θ. In the following, we assume a constant D_e (Nye and Marriott 1969). Thus, the rhizosphere domain is homogeneous, and concentrations are constant at $t = 0$ (Roose Fowler and Darrah 2001, Tournier Hecht and Comte 2015). The uptake by the root is given by the flux of the solutes at the soil–root interface, thus it is a function of the concentration in soil solution (C_l). In the rhizosphere, advection is negligible in many cases of nutrient uptake (Roose and Kirk 2008). In our scenarios, advection would increase the phosphorus uptake by ~3%, and ammonium uptake up to 6% for peak transpiration (Supplementary Material). Advection in these classical rhizosphere models also contradicts the mirroring root assumption without replenishment from a larger scale model (Kuppe et al. 2022b). We aim for validation of the model reduction, and for simplicity, we developed our approach for diffusive transport.

Uptake follows a nonlinear Michaelis–Menten curve, but nonlinearity in the boundary conditions introduces the need for iterations coming from, e.g. a Newton–Raphson method. To exclude numerical errors from such iterations, uptake is assumed to be in the linear part of the curve (Nye 1966):

$$q^* = \alpha C_l, \tag{6}$$

across the root surface and orthogonal to the root surfaces, $\boldsymbol{q} \cdot \mathbf{n}$, where $\mathbf{n}$ is the outward unit normal on the boundaries Γ_s and Γ_r, respectively. The root is a boundary, Γ_r, to the rhizosphere. This boundary includes the volumetric root hair. The other boundaries are symmetric (see geometry of Ω), hence, the zero-flux condition.

We solve the strong form, equation system (1)–(4), numerically using the FEM. The finite elements' local basis functions (polynomial functions) are continuous but not globally smooth (not differentiable across element boundaries), thereby they do not satisfy the strong form. The weak form of a partial differential equation (PDE) reduces the order of derivatives, and its solutions are required to exist within Sobolev spaces, H^1 (with weaker requirements on differentiability), which matches the FEM basis functions. Multiplying Eqn (1) with an arbitrary test function $\tilde{C} \in V = \{\tilde{C} \in H^1(\Omega) : \tilde{C}|_\Gamma = 0\}$ yields the weak form:

$$\int_\Omega \tilde{C} \left(\frac{\partial C}{\partial t} - \operatorname{div}(\boldsymbol{q}) - f \right) d\Omega = 0 . \tag{7}$$

Split the diffusion term in Eqn (7) due to integration by parts $\int_\Omega \tilde{C} \operatorname{div}(\boldsymbol{q})\, dV = \int_\Omega \operatorname{div}(\tilde{C}\boldsymbol{q})\, dV - \int_\Omega \nabla\tilde{C}\, \boldsymbol{q}\, d\Omega$ and apply the divergence theorem for the relationship $\int_\Omega \operatorname{div}(\tilde{C}\boldsymbol{q})\, dV = \int_\Gamma \tilde{C}\boldsymbol{q} \cdot \mathbf{n}\, d\Gamma = \int_{\Gamma_r} \tilde{C}\, q^* d\Gamma$ to obtain

$$\int_\Omega \tilde{C} \left(\frac{\partial C}{\partial t} - f \right) d\Omega + \int_\Omega \nabla\tilde{C}\, \boldsymbol{q}\, d\Omega - \int_{\Gamma_r} \tilde{C}\, q^*\, d\Gamma = 0 . \tag{8}$$

substituting q^*, C, and assuming $f = 0$ (no further reactions in the rhizosphere), Eqn (8) becomes

$$\int_\Omega D_e b\, \nabla\tilde{C} \cdot \nabla C_l\, d\Omega + \int_\Omega \tilde{C} b \frac{\partial C_l}{\partial t} d\Omega - \int_{\Gamma_r} \tilde{C}\, \alpha C_l\, d\Gamma = 0 . \tag{9}$$

For the discretization, we used tetrahedral finite elements. Thus, let T_h be the tetrahedralization of Ω, and the finite element subspace of V is denoted by $V_h = \{\tilde{C}_h \in C^0(\bar{\Omega}) : \tilde{C}_h|_{\Omega_e} \in P(\Omega_e)\ \forall \Omega_e \in T_h,\ \tilde{C}_h|_\Gamma = 0\}$, where P is the set of polynomials of a certain degree. Since C^0 denotes the set of continuous functions, we switch notations for C_l to C_h in the discrete form, for convenience, to reduce indices. We seek to find

$$C_h \in V_h : \int_\Omega D_e b\, \nabla\tilde{C}_h \cdot \nabla C_h\, d\Omega + \int_\Omega \tilde{C}_h b \frac{\partial C_h}{\partial t} d\Omega - \int_{\Gamma_r} \tilde{C}_h\, \alpha C_h\, d\Gamma = 0 \quad \forall \tilde{C}_h \in V_h . \tag{10}$$

With continuous time gradient on T_h, it is a so-called line-method, and the time stepping is described later.

Instead of meshing the full rhizosphere domain around a cm root, the rhizosphere is split into symmetric sections as drawn in Fig. 2A and B. Thus, the 3D geometry of the rhizosphere domain Ω describes a slice of the cylindrical root surface containing a

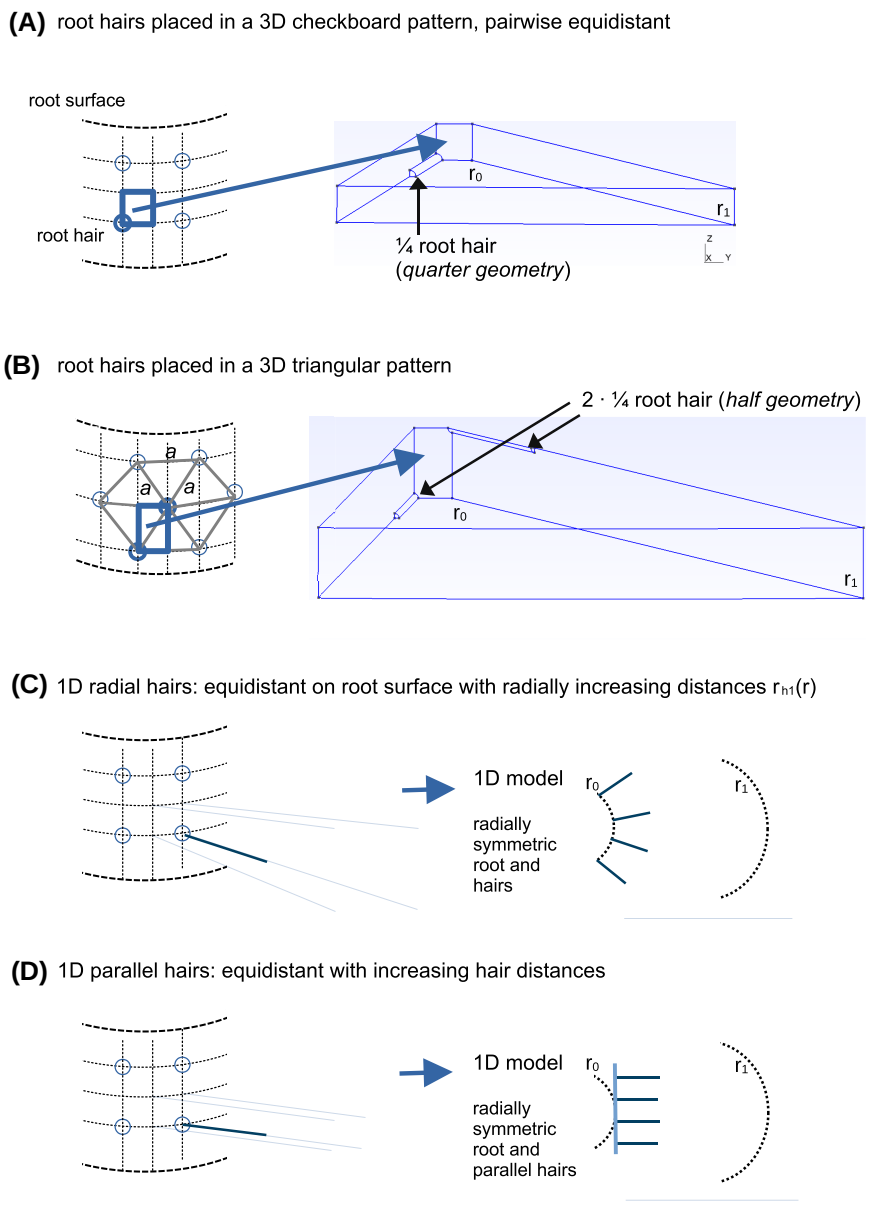

Figure 2 Idealized 3D models (A, B) and 1D approximations (C, D). Left: the root surface with the placement of root hairs. Right: the model representation of the rhizosphere domain. The notation 'a' in (B) indicates equal length of $2r_{h1}$.

quarter of one or two root hairs (*quarter-* and *half geometry*) and spanning to the mid-distance to the neighbouring hair (Fig. 2A and B). To ensure symmetry, the surfaces at the cutting planes were implemented using a zero-flux (homogeneous Neumann) boundary condition, Eqn (2). The mesh generator Gmsh was used to create (1) the geometry and (2) the mesh files in 3D, which are imported into our code (Geuzaine and Remacle 2009). Fine root hairs require a sufficiently fine mesh locally, and the number of nodes can be quite large.

Uptake over one cm root and the root hairs surface is (assuming that the uptake properties of the root and root hairs are the same)

$$U(t) = \int_0^t \int_{\Gamma_r} \alpha C_l \, d\Gamma ds \,. \tag{11}$$

Using the quarter and half geometries (Fig. 2A and B) to obtain the uptake of a unit cm root, this cumulative uptake U must be multiplied by $4N_h$ and $2N_h$, respectively, where N_h is the number of root hairs on the surface of a unit cm root.

We provide the code for the 3D simulation (https://doi.org/10.26165/JUELICH-DATA/I589IG), including the meshes and the FEM implemented in Julia/Gridap.jl (Geuzaine and Remacle 2009, Badia and Verdugo 2020, Verdugo and Badia 2022). Alternatively, we tested the C++ sub-language FreeFem++ (Hecht 2012), which produced the same results as the Julia code (not shown further). High-level programming codes have the advantage that the user does not have to deal with the programming of the finite element system itself, including the so-called stiffness matrix on a lower level, but can use the functional forms directly in the code.

2.2 Transport in the rhizosphere in 1D: root hairs as reaction term

The previous equation system is now represented in radial coordinates, and the root hairs do not belong to the boundary but are a sink term inside the domain $\Omega_{1D} \subset \mathbb{R}$. The boundary, $\Gamma_{1D} = \partial\Omega_{1D} = r_0 \cup r_1$, is the root radius, r_0, and the outer radius, typically denoted as r_1. The diffusion equation of a substance with concentration in soil solution C_l: $\mathbb{R} \times [0, T] \rightarrow \mathbb{R}$ is

$$b\frac{\partial C_l}{\partial t} - \frac{1}{r}\frac{\partial}{\partial r}\left(rD_e b\frac{\partial C_l}{\partial r}\right) = -I_h \quad \text{in } \Omega_{1D} \times (0, T] \tag{12}$$

$$\frac{\partial C_l}{\partial r} = 0 \quad \text{at } r_1 \times (0, T] \tag{13}$$

$$D_e b\frac{\partial C_l}{\partial r} = q^* \quad \text{at } r_0 \times (0, T] \tag{14}$$

$$C_l(r, 0) = C_0 \quad \text{in } \Omega_{1D}, \tag{15}$$

where I_h is the volumetric root-hair-uptake term calculated in the transient Eqn (12) from a (stepwise) steady-state diffusion profile over r (Eqn iii: Baldwin et al. 1973) and discretized as in Kuppe et al. (2021). In the numerical solving of this PDE, the diffusion profile around root hairs, used to calculate I_h, is iteratively updated over time and it follows the transient solute concentrations in the rhizosphere. The time-steps are small for convergence, and in the case macroscopic events reach the rhizosphere, the steady-state approximation follows these new updated conditions, while transient approaches would need to carefully implement how to update the transient root hair models. Alternative options for I_h, which do not rely on a steady-state assumption, were proposed by Leitner et al. (2010a). Using the method of homogenization, they derived three cases. The first case is applicable when the rates of uptake by hairs and diffusion are comparable; a sink term for root hair uptake is provided that considers a dynamic development of a depletion zone within the root hair zone, as well as the impedance of diffusion caused by the presence of the root hairs. The other two cases represent situations where uptake by root hairs is negligibly small or uptake by root hairs is large enough that all solutes within the root hair zone are taken up quickly, such that the root hairs essentially extend the root radius by the root hair length (this corresponds to the model proposed by Passioura 1963). We did not implement these cases and tested them here, but rather stuck to the more commonly used steady-state estimation of I_h.

We call the sink from root hairs 'upscaled' to the larger root segment scale, because the vertical dimension for the diffusion of solutes towards root hairs is reduced. The root hair uptake per surface area of root hairs according to Baldwin et al. (1973),

$$I_h = \alpha A_h C_{lr}, \tag{16}$$

uses the solute concentration at the root hair surface,

$$C_{lr} = C_l / \left(1 - \frac{\alpha\, r_h}{2D_e b} + \frac{\alpha\, r_h r_{h1}^2}{D_e b(r_{h1}^2 - r_h^2)}\ln\left(\frac{r_{h1}}{r_h}\right)\right), \tag{17}$$

where A_h (cm^2 cm^{-3}) is the root hair surface area per unit soil volume, which is nonzero for the length of the root hairs l_h, and r_h is the root hair radius. The volumetric surface area, A_h, is computed from the number of hairs, N_h (cm^{-1} root), defined per cm root of radius r_0, and this is discretized when implementing (Kuppe et al. 2021).

The mid-distance to the neighbouring root hairs, r_{h1}, is modelled as increasing with r (Fig. 2C) as $r_{h1}(r) = \sqrt{\pi r/(2N_h)}$, or constant (Fig. 2D) as $r_{h1} = r_{h1}(r_0)$. Figure 2D shows a geometry where the root surface is rolled out so that Cartesian coordinates apply, and the root hair zone can be described by a rectangular domain (see, e.g. Leitner et al. 2010a). Note that this representation only simplifies the radial coordinate system for the root hair sink term, not the rest of the transport equation.

The rhizosphere in the 1D and 3D models inter-root competition for nutrient uptake with a zero-flux outer boundary (Neumann boundary). In comparison, Eqn (17) in the 1D model is the steady-state solute concentration at the root hair surface from a concentration profile (influx equal to outflux) between the root hair surface and the mid-point of neighbouring root hairs for a given uptake flux and concentration at the outer boundary (Dirichlet boundary). The Dirichlet boundary for the diffusion profile normal to the root hair length is necessary to obtain a non-trivial solution that is not zero concentration in the rhizosphere. The concentration at the Dirichlet boundary on the root hair scale is implicitly calculated in the integral below obtaining Eqn (17), which depends on the average concentration (C_l) between root hair surface and mid-distance to the neighbouring hair according to the steady-state diffusion towards the root hair surface:

$$C_l\pi(r_{h1}^2 - r_h^2) = \int_{r_h}^{r_{h1}} 2\pi r_\perp C_\perp dr_\perp = \int_{r_h}^{r_{h1}} 2\pi r_\perp C_{lr}\left(1 + \frac{\alpha r_h}{D_e b}\ln\left(\frac{r_\perp}{r_h}\right)\right)dr_\perp,$$

where $r_\perp$ and $C_\perp$ are the coordinate and solution concentration around a root hair (orthogonal), which is in steady-state $C_\perp(r_\perp) = C_{lr}\left(1 + \frac{\alpha r_h}{D_e b}\ln\left(\frac{r_\perp}{r_h}\right)\right)$ (compare with Baldwin et al. 1973). Integration results in Eqn (17).

At the boundary $r_\perp = r_{h1}$ it holds $C_\perp(r_{h1}) = C_{lr}\left(1 + \frac{\alpha r_h}{D_e b}\ln\left(\frac{r_{h1}}{r_h}\right)\right)$, which is an increasing function ($r_{h1} > r_h$). Hence, when the average concentration is a given value, coming from the diffusion on the root segment scale, the concentration at the root hair surface, C_{lr}, becomes smaller for increasing r_{h1} (Fig. 3).

The cumulative uptake of a root segment of unit-length in 1D radial coordinates (compare with Eqn 11) is computed by

$$U(t) = 2\pi\alpha\int_0^t \left(r_0 C(r_0, s) + N_h\int_{r_0}^{r_0+l_h} r_h C_{lr}(r, s)dr\right)ds, \tag{18}$$

which is the sum of uptake by the surface of the main root and root hairs, where C_{lr} (Eqn 17) is the solute concentration at the root hairs from the diffusion around hairs (overview of main symbols see Tables 1–3).

2.3 The root and root hairs as point sink in the rhizosphere

We ask whether the model can be reduced further. Therefore, we investigate how the numerical solution from a 0D point sink behaves compared with the root as a rhizosphere boundary (Fig. 4C and D). A point sink is a localized sink of a quantity that is concentrated at a single point in the spatial domain, which can be represented by a Dirac delta function. This approach is numerically challenging as the concentration at the source/sink goes to infinity, and it affects the optimal mesh size.

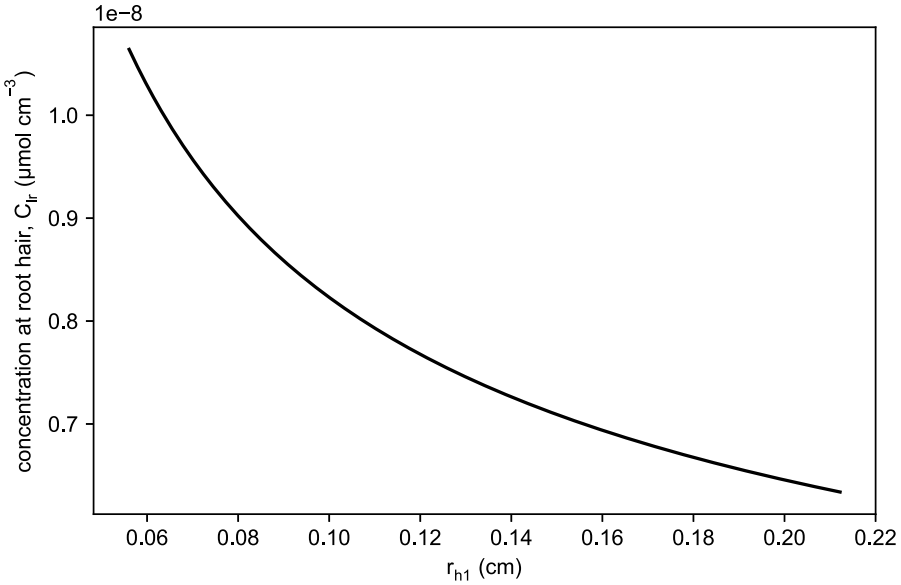

Figure 3 The concentration at the root surface (C_{lr}, Eqn 17) for increasing mid-distances to neighbouring root hairs, r_{h1}, with $r_h = 0.005$ cm, $N_h = 15$, $C_l = P_0$, uptake and soil values for the phosphorus case, Table 2.

Table 1 List of variables and symbols.

C	Nutrient concentration in whole soil, $C = bC_l$
C_l	Solute concentration
C_h	C_l in the discrete form, Eqn (10)
Ω	Rhizosphere section, computational domain
Ω_e	Finite element, $\Omega_e \in T_h$
T_h	Tetrahedralization of Ω
Γ_s	Soil boundary, symmetric intersections (outer boundary)
Γ_r	Root surface (inner boundary)
C_{lr}	Solute concentration at the root hair surface
$C_\perp$	Solute concentration orthogonal to the root hair
$r_\perp$	Radial distance from root hair, orthogonal to r
r_{h1}	Mid-distance to the neighbouring root hair
I_h	Nutrient uptake by root hairs

We reduced the 3D cylinder to a 2D disc, which has the same result due to symmetry in the axial direction of the root, just as in the 1D radial model. The equation system becomes

$$\frac{\partial C}{\partial t} - \mathrm{div}(\boldsymbol{q}) + \delta(\mathrm{x} - \mathrm{x}_0)2\pi(r_0\mathrm{L} + r_h N_h \mathrm{L}\, l_h)\alpha C_l = 0 \text{ in } \Omega \times (0, T] \quad (19)$$

$$\boldsymbol{q} \cdot \mathbf{n} = 0 \text{ on } \Gamma \times (0, T] \quad (20)$$

$$C_l(\mathrm{x}, 0) = C_0 \text{ in } \Omega, \quad (21)$$

where L in Eqn (18) is the unit-length of a root segment (1 cm), r_0, r_h, N_h, root radius (cm), root hair radius (cm), and number of hairs per cm root (cm^{-1}), respectively, as above, and δ is the Dirac delta (cm^{-2}) with $\mathrm{x} = (x, y)$ and position $\mathrm{x}_0 = (0, 0)$, which will be included in the bilinear form when implementing to represent the point sink of the root and root hairs instead of the flux over the boundary.

Table 2 Parameter values for phosphorus and ammonium.

		Phosphorus	Ammonium	
Soil buffer power	b	1000	100	Unitless
Self-diffusion	D_l	8.9e−6	1.6e−5	cm^2 s^{-1}
Effective diffusion in soil	D_e	8.9e−10	1.6e−8	cm^2 s^{-1}
Absorption coefficient of the root	α	1e−4	1e−5	cm s^{-1}
Initial concentration in soil solution	C_0	1e−3	1	mM

Table 3 Parameter values for the root geometry.

Root radius	r_0	0.03	cm
Rhizosphere radius	r_1	0.43	cm
Root hair radius	r_h	0.0005; 0.005	cm
Root hair length	l_h	0.03; 0.3	cm
Root hair number	N_h	15; 1500	cm^{-1}

2.4 Meshing and simulations

The problem definition is symmetric, and we used this property to reduce the degree of freedom (i.e. the size) of the mesh, significantly speeding up the simulation time. This symmetric geometry is a slice of rhizosphere from r_0 to r_1 and part of a root hair to the mid-distance of root hairs, which is obtained with a Gmsh script. In the Gridap code, we imported a Gmsh mesh in '.msh' format (note that for the simulation run with FreeFem++, we imported an INRIA medit mesh format, but we continued with Gridap for the plots; specifically, Gridap.jl 0.19.1, GridapGmsh.jl 0.7.3, with Julia v1.11.5, and Gmsh 4.13.1).

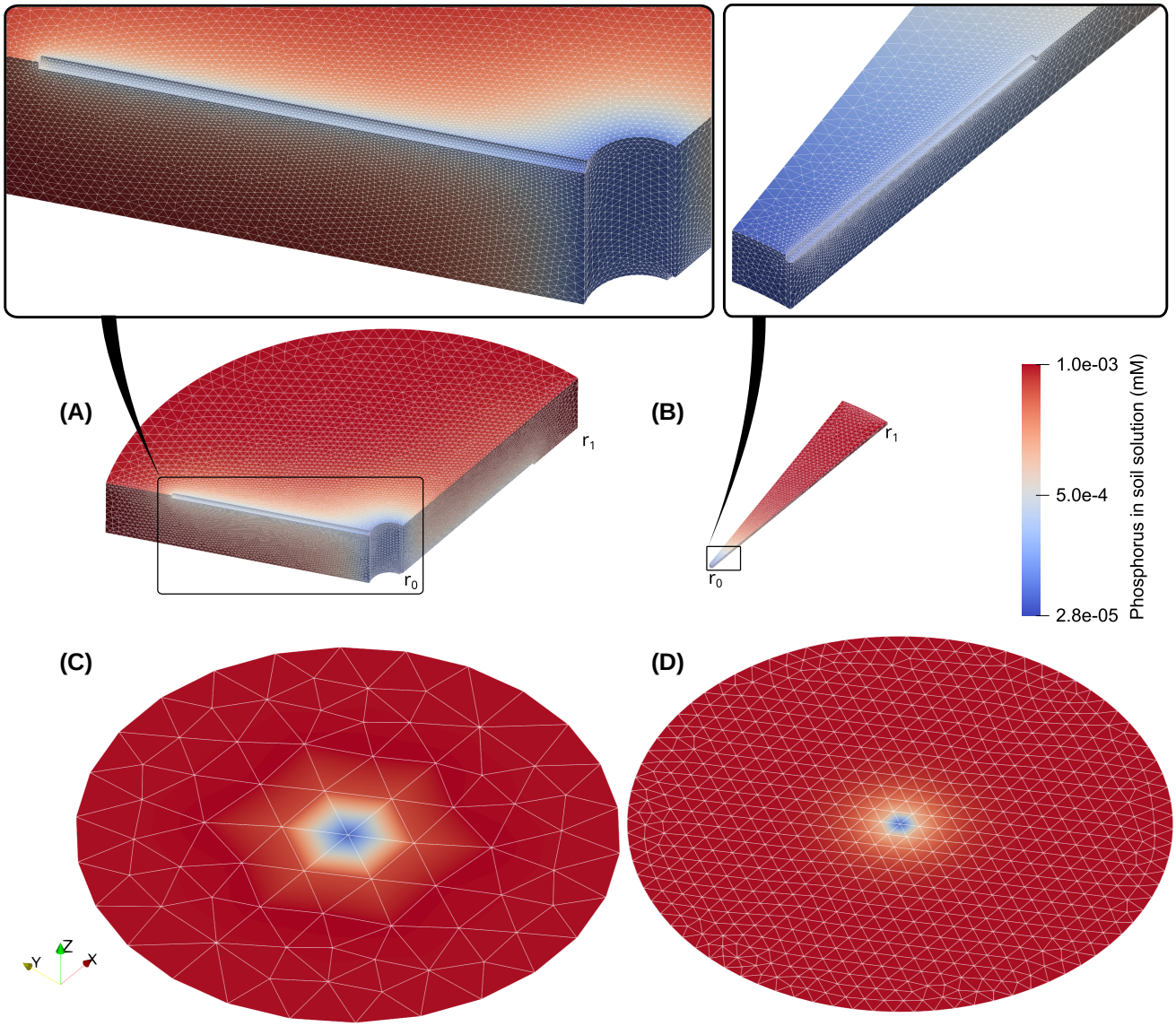

Figure 4 Phosphorus concentration in the soil solution around part of the root and root hair. Slices from $r_0 = 0.03$ cm and $r_1 = 0.43$ cm are with an exemplary (A) long-thick-coarse root hair distribution: $N_h = 15$, $l_h = 0.3$ cm, $r_h = 0.005$ cm with the triangularly spaced root hair pattern, i.e. quarters of root hairs are in the upper left and lower right corners; and (B) a short-thin-dense root hair distribution: $N_h = 1500$, $l_h = 0.03$ cm, $r_h = 0.0005$ cm, equidistant checkboard pattern, i.e. a quarter of a root hair is in the lower right corner. (C, D) Point sink in for a 2D mesh with size 0.1 cm and 0.03 cm, respectively.

We used the BDF method from Julia/gridap.jl (the associated DIRK tableau), which is currently fixed-step with $\Delta t = 2\text{e}{-6}$ d, and we also used a BDF method in the 1D code. However, using an adaptive solver with a small starting time-step of 1e−10 d. We verified convergence by testing finer meshes and time-steps for the influence of numerical errors. Therefore, it was justified that we perform a validation of the model assumptions rather than a comparison of numerical solvers (Fig. 1). In a mesh that was refined by splitting with Gmsh, e.g. for the case $N_h = 1500$ and $l_h = 0.03$ cm, $r_h = 0.0005$ cm, the cumulative uptake changed by <0.2%.

We also verified conservation of mass. We compared the fluxes over the boundaries in the time loop $U = \sum_t \Delta t \sum_{\Gamma_2} \int_{\Gamma_e} \alpha C_h \, d\Gamma_2 \times \mathrm{m}\, N_h$ (note C_h from Eqn 10) with the end amount of nutrient in the rhizosphere ($\int \mathrm{m} N_h b C_T$) minus the initial amount: $\sum_{\Omega_e \in T_h} \int_{\Omega_e} C_0 - C_T \, d\Omega \times b\, \mathrm{m} N_h$, where $m = 2$ for the triangular equidistant case and $m = 4$ for the checkboard pattern case.

We tested extreme cases to cover all possible scenarios, including a scenario that reflects fine root branches: coarse and dense root hair distributions on the root surface, $N_h \in \{15,\ 1500\}$, which can be (artificially) long or, as usual, short, $l_h \in \{0.3,\ 0.03\}$ cm. We define that when root hairs are coarsely distributed, they are thick with root hair radius $r_h = 0.005$ cm, like very fine lateral roots, and dense hairs are thin $r_h = 0.0005$ cm. The soil parameters are $\tau = 0.25$ for the tortuosity factor, $\theta = 0.4$ for the volumetric water content,

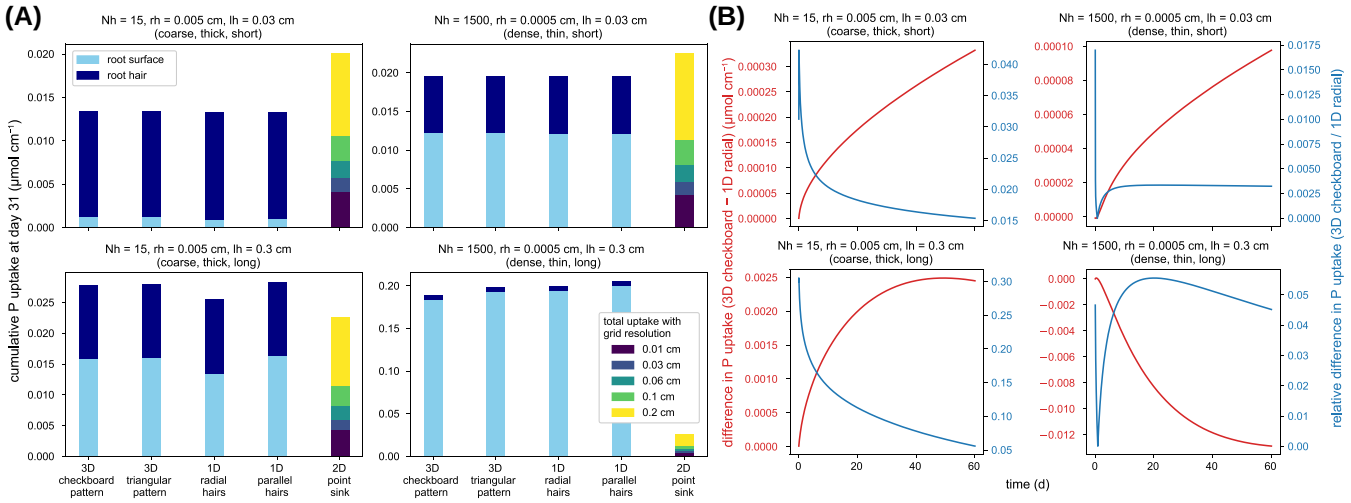

Figure 5 Comparison of the four cases for phosphorus (P) uptake: short and long in the rows ($l_h = 0.03$ cm, 0.3 cm), and thick-coarse ($N_h = 15$, $r_h = 0.005$ cm), thin-dense in the columns ($N_h = 1500$, $r_h = 0.0005$ cm) root hairs for the simulations of phosphorus uptake. (A) Phosphorus uptake after simulation day 31 divided over the parent root surface (light-blue, bottom bars) and the root hairs (dark-blue, top bars) on a unit cm root. The solutions of the root as point-sink in a 2D mesh, colours indicate how much more uptake is simulated with a coarser mesh resolution. (B) The absolute (red) and the relative differences (blue) over the simulated uptake-time of the 1D radial and the 3D checkboard pattern.

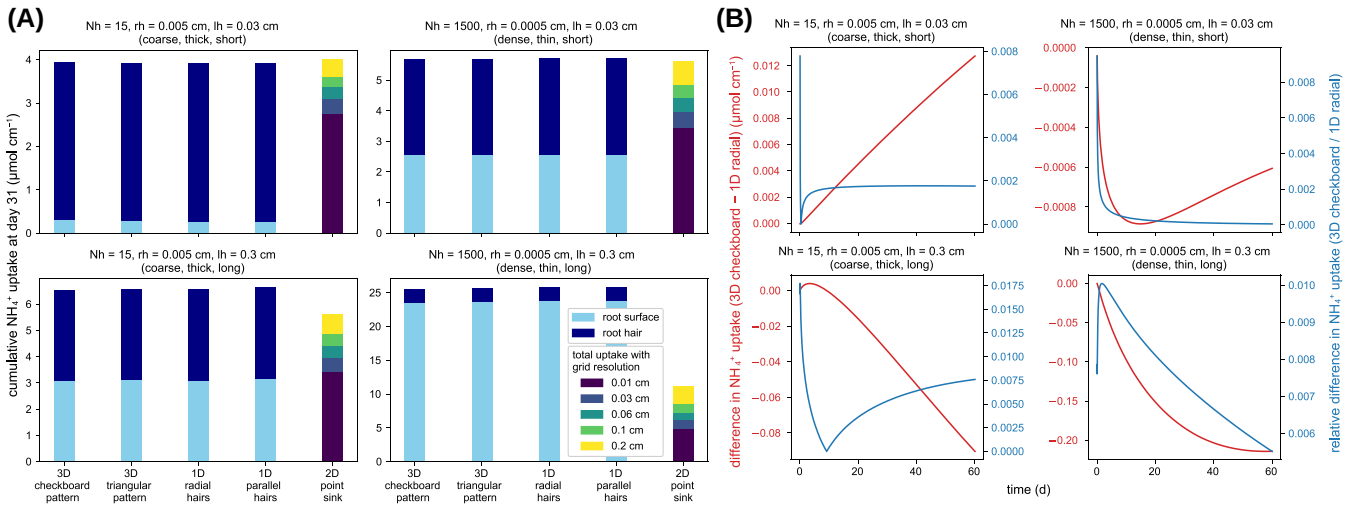

Figure 6 Comparison of the four cases for ammonium (NH_4^+) uptake: short and long in the rows ($l_h = 0.03$ cm, 0.3 cm), and thick-coarse ($N_h = 15$, $r_h = 0.005$ cm), thin-dense in the columns ($N_h = 1500$, $r_h = 0.0005$ cm) root hairs for the simulations of ammonium uptake. (A) NH_4^+ uptake after simulation day 31 divided over the parent root surface (light-blue, bottom bars) and the root hairs (dark-blue, top bars) on a unit cm root. The solutions of the root as point-sink in a 2D mesh, colours indicate how much more uptake is simulated with a coarser mesh resolution. (B) The absolute (red) and the relative differences (blue) over the simulated uptake-time of the 1D radial and the 3D checkboard pattern.

and $D_e = D_l \theta \tau / b$ for the effective diffusion coefficient (Table 2). Phosphorus can often be strongly sorbed to the soil, for example, in Andosols or Oxisols (Oburger Jones and Wenzel 2011, Kuppe et al. 2022a). Here, the solutes are strongly sorbed, and the soil buffer power is in the higher range (like for phosphorus in Oxisols), but not as high as the soil buffer power for phosphorus in Andosols. The main root radius and mid-distance to a neighbouring root are $r_0 = 0.03$ cm and $r_1 = 0.43$ cm, respectively (Table 3). Figure 4 shows meshes and concentrations.

3. Results and conclusions

Overall, 1D and 3D models simulate very similar uptake; however, there are nuances in the low diffusion case of phosphorus (Fig. 5A), especially for the 1D model with radial root hairs (Fig. 5B). The 0D root-sink model performed badly, with results strongly depending on chosen grid resolution.

The 1D model with parallel hairs (without increasing the root hair mid-distance) over-estimates phosphorus uptake, which is explained by the constant and small value of r_{h1},

resulting in greater C_{lr} (Eqn 17, Fig. 3) and thus I_h. Although the parallel root hair model gives results closer to the 3D model, it is still geometrically not correct in respect to the hairs. The main root geometry is radial in all models 1D.

In contrast to the 'parallel hairs' model, the radial hair mid-distance model deviates stronger from the 3D model. It under- and over-estimates depending on the root geometrical parameters. Figure 5B shows how the error of this model develops over time. The difference relative to the total simulated uptake decreases over time, which may generally be good because the rhizosphere was not yet fully depleted. Growing root systems tend to have many young roots and thus the root system uptake is likely to be sensitive to early errors. After 20 days the model deviated up to 10%. Long and thick root hairs had the largest relative differences. However, the case with $l_h = 0.3$ cm is also an extreme one, which may represent fine lateral roots rather than hairs, having 4.5 cm of those thicker hairs on the 1 cm main root. Note that we compared uptake, not the concentration gradients along the root hairs directly, and the error corrects itself over time as the rhizosphere converges to a steady-state. The differences in nutrient concentration gradients and uptake along the root hairs are more pronounced for thicker root hairs.

The 0D root-sink model performs badly. Depending on the grid resolution, it over or underestimates phosphorus uptake. Note that the two cases: '$N_h = 1500$, $r_h = 0.0005$, $l_h = 0.03$' and '$N_h = 15$, $r_h = 0.005$, $l_h = 0.3$' have the same root surface area. That causes the same uptake for the 0D point sink for both scenarios, but not for the 1D and 3D model geometries.

For the scenario with fast diffusion (ammonium), the 1D and 3D models give similar uptake (Fig. 6A). The absolute difference in uptake can increase, but the relative difference drops quickly and is below 1% even for the worst model representation (Fig. 6B). The total uptake by the point sink root model was lower than the 3D reference. Again, simulated uptake depends on the mesh size (Figs 5A and 6A) with the coarser mesh simulating more uptake and thereby getting closer to the reference solution. The mesh resolution can be tuned to match the corresponding uptake strength of root and root hairs. For example, Lu et al. (2024) used coarse 15×15 cm volumes and a Michaelis–Menten uptake kinetics for nitrogen in the volumes, which is a similar approach to the point sink presented here. We may suggest an element size of approximately half the rhizosphere radius for the tested scenarios. However, obtaining a closer approximation for the '0D point sink' case by selecting a specific mesh resolution (e.g. $r_1/2$) does not indicate general applicability but its nonphysical nature and dependence on spatial discretization.

We note that in Figs 5A and 6A, the upper right subplot (dense, short, and thin hairs) is the usual root hair scenario, and uptake of nitrogen was estimated well. Our model was limited to the uptake of a single nutrient under constant water conditions, neglecting soil water dynamics, convective solute transport, multiple nutrients, and nonlinear uptake and sorption. Future models can use or extend the 3D code and benchmark it against other models, as was done for water flow and uptake in functional–structural plant models (compare benchmark C1.1, Schnepf et al. 2023). The 3D code is available online for benchmarking further scenarios and comparing 1D rhizosphere models against a 3D reference.

Based on the overall good agreement between 1D and 3D models in most but some extreme cases, we conclude that the upscaling of root hairs to the rhizosphere transport scale used in the 1D diffusion model is a viable way to simulate uptake by roots with root hairs. This approach helps in avoiding computational limitations. Reducing roots or root hairs to sink terms can become problematic at larger radii.

Acknowledgements

We thank Alexandre Magueresse from the Gridap developers.

Supplementary material

Supplementary material is available at *In Silico Plants* online.

Conflicts of interest

None declared.

Funding

Open access fees were funded by the Deutsche Forschungsgemeinschaft (DFG, German Research Foundation)—491111487. C.W.K. and J.A.P. were institutionally funded by the Helmholtz Association (POF IV: 2171, Biological and environmental resources for sustainable use) and by the Root2Res Project, which has received funding from the European Union's Horizon Europe research and innovation programme under grant Agreement no. 101060124. A.S. acknowledges funding by the project 'RhizoWheat' (grant 031B1413B) in the framework of the funding initiative 'Rhizo4Bio (Phase 2)' of the German Federal Ministry of Education and Research (BMBF).

Data availability

The simulation results underlying this article will be shared on reasonable request. The FEM code and the meshes are available under an MIT licence and shared on Jülich DATA, https://doi.org/10.26165/JUELICH-DATA/I589IG.

References

Badia S, Verdugo F. Gridap: an extensible finite element toolbox in Julia. *J Open Source Softw* 2020;**5**:2520. https://doi.org/10.21105/joss.02520

Baldwin JP, Nye PH, Tinker PB. Uptake of solutes by multiple root systems from soil. *Plant Soil* 1973;**38**:621–35. https://doi.org/10.1007/BF00010701

Barber S, Cushman J. Nitrogen uptake model for agronomic crops. In: *Modeling Wastewater Renovation: Land Treatment*. New York: Wiley Interscience, 1981, 382–489.

Bhat KKS, Nye PH, Baldwin JP. Diffusion of phosphate to plant roots in soil. *Plant Soil* 1976;**44**:63–72. https://doi.org/10.1007/BF00016955

Claassen N, Barber SA. Simulation model for nutrient uptake from soil by a growing plant root system. *Agron J* 1976;**68**:961–4. https://doi.org/10.2134/agronj1976.00021962006800060030x

Claassen N, Syring KM, Jungk A. Verification of a mathematical model by simulating potassium uptake from soil. *Plant Soil* 1986;**95**:209–20. https://doi.org/10.1007/BF02375073

Cushman JH. An analytical solution to solute transport near root surfaces for low initial concentration: I. Equations development. *Soil Sci Soc Am J* 1979;**43**:1087–90. https://doi.org/10.2136/sssaj1979.03615995004300060005x

Daly KR, Keyes SD, Masum S *et al.* Image-based modelling of nutrient movement in and around the rhizosphere. *J Exp Bot* 2016;**67**:1059–70. https://doi.org/10.1093/jxb/erv544

Geelhoed JS, Mous SLJ, Findenegg GR. Modeling zero sink nutrient uptake by roots with root hairs from soil: comparison of two models. *Soil Sci* 1997;**162**:544–53. https://doi.org/10.1097/00010694-199708000-00003

Geuzaine C, Remacle J-F. Gmsh: a 3-D finite element mesh generator with built-in pre- and post-processing facilities. *Int J Numer Methods Eng* 2009;**79**:1309–31. https://doi.org/10.1002/nme.2579

Gonzalez D, Postma J, Wissuwa M. Cost-benefit analysis of the upland-rice root architecture in relation to phosphate: 3D simulations highlight the importance of S-type lateral roots for reducing the pay-off time. *Front Plant Sci* 2021;**12**:641835. https://doi.org/10.3389/fpls.2021.641835

Hecht F. New development in freefem++. *J Numer Math* 2012;**20**:251–65. https://doi.org/10.1515/jnum-2012-0013

Itoh S, Barber SA. Phosphorus uptake by six plant species as related to root hairs. *Agron J* 1983;**75**:457–61. https://doi.org/10.2134/agronj1983.00021962007500030010x

Keyes SD, Daly KR, Gostling NJ *et al.* High resolution synchrotron imaging of wheat root hairs growing in soil and image based modelling of phosphate uptake. *New Phytol* 2013;**198**:1023–9. https://doi.org/10.1111/nph.12294

Kuppe CW, Huber G, Postma JA. Comparison of numerical methods for radial solute transport to simulate uptake by plant roots. *Rhizosphere* 2021;**18**, 100352. https://doi.org/10.1016/j.rhisph.2021.100352

Kuppe CW, Kirk GJD, Wissuwa M *et al.* Rice increases phosphorus uptake in strongly sorbing soils by intra-root facilitation. *Plant Cell Environ* 2022a;**45**:884–99. https://doi.org/10.1111/pce.14285

Kuppe CW, Schnepf A, von Lieres E *et al.* Rhizosphere models: their concepts and application to plant–soil ecosystems. *Plant Soil* 2022b;**474**:17–55. https://doi.org/10.1007/s11104-021-05201-7

Leitner D, Klepsch S, Ptashnyk M *et al.* A dynamic model of nutrient uptake by root hairs. *New Phytol* 2010a;**185**:792–802. https://doi.org/10.1111/j.1469-8137.2009.03128.x

Leitner D, Schnepf A, Klepsch S *et al.* Comparison of nutrient uptake between three-dimensional simulation and an averaged root system model. *Plant Biosyst—An Int J Deal All Aspects Plant Biol* 2010b;**144**:443–7. https://doi.org/10.1080/11263501003726334

Lu J, Lankhost JA, Stomph TJ *et al.* Root plasticity improves maize nitrogen use when nitrogen is limiting: an analysis using 3D plant modelling. *J Exp Bot* 2024;**75**:5989–6005. https://doi.org/10.1093/jxb/erae298

Ma Z, Walk TC, Marcus A *et al.* Morphological synergism in root hair length, density, initiation and geometry for phosphorus acquisition in *Arabidopsis thaliana*: a modeling approach. *Plant Soil* 2001;**236**:221–35. https://doi.org/10.1023/A:1012728819326

Macariola-See N, Woodard HJ, Schumacher T. Field verification of the Barber–Cushman mechanistic phosphorus uptake model for maize. *J Plant Nutr* 2003;**26**:139–58. https://doi.org/10.1081/PLN-120016501

Mai TH, Schnepf A, Vereecken H *et al.* Continuum multiscale model of root water and nutrient uptake from soil with explicit consideration of the 3D root architecture and the rhizosphere gradients. *Plant Soil* 2019;**439**:273–92. https://doi.org/10.1007/s11104-018-3890-4

Mollier A, De Willigen P, Heinen M *et al.* A two-dimensional simulation model of phosphorus uptake including crop growth and P-response. *Ecol Model* 2008;**210**:453–64. https://doi.org/10.1016/j.ecolmodel.2007.08.008

Nye PH. The effect of the nutrient intensity and buffering power of a soil, and the absorbing power, size and root hairs of a root, on nutrient absorption by diffusion. *Plant Soil* 1966;**25**:81–105. https://doi.org/10.1007/BF01347964

Nye PH, Marriott FHC. A theoretical study of the distribution of substances around roots resulting from simultaneous diffusion and mass flow. *Plant Soil* 1969;**30**:459–72. https://doi.org/10.1007/BF01881971

Oburger E, Jones DL, Wenzel WW. Phosphorus saturation and pH differentially regulate the efficiency of organic acid anion-mediated P solubilization mechanisms in soil. *Plant Soil* 2011;**341**:363–82. https://doi.org/10.1007/s11104-010-0650-5

Passioura JB. A mathematical model for the uptake of ions from the soil solution. *Plant Soil* 1963;**18**:225–38. https://doi.org/10.1007/BF01347877

Postma JA, Kuppe C, Owen MR *et al.* OpenSimRoot: widening the scope and application of root architectural models. *New Phytol* 2017;**215**:1274–86. https://doi.org/10.1111/nph.14641

Roose T, Fowler AC, Darrah PR. A mathematical model of plant nutrient uptake. *J Math Biol* 2001;**42**:347–60. https://doi.org/10.1007/s002850000075

Roose T, Kirk GJD. The solution of convection–diffusion equations for solute transport to plant roots. *Plant Soil* 2008;**316**:257–64. https://doi.org/10.1007/s11104-008-9777-z

Ruiz S, Koebernick N, Duncan S *et al.* Significance of root hairs at the field scale—modelling root water and phosphorus uptake under different field conditions. *Plant Soil* 2020;**447**:281–304. https://doi.org/10.1007/s11104-019-04308-2

Schnepf A, Black CK, Couvreur V *et al.* Collaborative benchmarking of functional–structural root architecture models:

quantitative comparison of simulated root water uptake. *In Silico Plants* 2023;**5**:diad005. https://doi.org/10.1093/insilicoplants/diad005

Schnepf A, Leitner D. FEM simulation of below ground processes on a 3-dimensional root system geometry using distmesh and comsol multiphysics. *Proc ALGORITMY* 2009:321–30.

Schnepf A, Leitner D, Klepsch S. Modeling phosphorus uptake by a growing and exuding root system. *Vadose Zone J*. 2012; **11**:vzj2012.0001. https://doi.org/10.2136/vzj2012.0001

Schnepf A, Leitner D, Landl M *et al.* CRootBox: a structural–functional modelling framework for root systems. *Ann Bot* 2018;**121**:1033–53. https://doi.org/10.1093/aob/mcx221

Tournier P-H, Hecht F, Comte M. Finite element model of soil water and nutrient transport with root uptake: explicit geometry and unstructured adaptive meshing. *Transp Porous Med* 2015;**106**:487–504. https://doi.org/10.1007/s11242-014-0411-7

Verdugo F, Badia S. The software design of Gridap: a finite element package based on the Julia JIT compiler. *Comput Phys Commun* 2022;**276**:108341. https://doi.org/10.1016/j.cpc.2022.108341

Williams KA, McKay Fletcher DM, Petroselli C *et al.* A 3D image-based modelling approach for understanding spatio-temporal processes in phosphorus fertiliser dissolution, soil buffering and uptake by plant roots. *Sci Rep* 2022;**12**: 15891. https://doi.org/10.1038/s41598-022-19047-1